Journal of Applied Electrochemistry (2006) 36:105–113
DOI 10.1007/s10800-005-9046-2

Electrodeposition and corrosion behaviour of a Ni–W–B amorphous alloy

R. A. C. SANTANA[1], S. PRASAD[1,*], A. R. N. CAMPOS[1], F. O. ARAÚJO[1], G. P. DA SILVA[2] and P. DE LIMA-NETO[2]
[1]*Department of Chemical Engineering, CCT, Universidade Federal de Campina Grande, Post box 10108, CEP 58109-970, Campina Grande, PB, Brazil*
[2]*Department of Physical and Analytical Chemistry, Universidade Federal do Ceará, 6035, CEP 60455-970, Fortaleza, CE, Brazil*
*(*author for correspondence, fax: +55-83-310-1114, e-mail: prasad@deq.ufcg.edu.br)*

Received 6 July 2004; accepted in revised form 26 July 2005

Key words: alloy electrodeposition, amorphous structures, corrosion, electrodeposited films, Ni–W–B alloy

Abstract

Electrodeposition of Ni–W–B alloys from plating baths containing ammonia and citrate is reported. Optimum conditions for plating including current density, temperature, mechanical agitation and pH were studied. The corrosion resistance and amorphous character were also evaluated. The operational conditions for depositing the alloy with good corrosion resistance were: current density 35 mA cm^{-2}, bath temperature 40 °C, pH 9.0 and cathode rotation at 90 rpm. The alloy was deposited at 38% current efficiency, with an average composition of 73 wt% Ni, 27 wt% W and traces of boron and with E_{corr} −0.300 V and R_p 3.369×10^4 Ω. The deposit obtained under these conditions had an amorphous character with the presence of some microcracks on its surface reaching down to the copper substrate. Electrochemical corrosion tests verified that the Ni–W–B alloy had better corrosion resistance than Co–W–B.

1. Introduction

Compared to the electrodeposition of a single metal, alloys are denser, harder, generally more resistant to corrosion, possess better magnetic properties and are suited to subsequent coating by electrodeposition [1].

Tungsten deposits are of interest because of their unusual combination of properties. Electrodeposition of tungsten in the pure state has not yet been successful from either aqueous or organic solutions. But no experimental difficulty is experienced in codepositing tungsten with the group 8 metals. Several authors have investigated the process of electrodeposition of tungsten with iron group metals in aqueous solutions [2–6]. It is well known that alloys such as Co–W–B and Ni–W–B are characterized by high surface hardness; Vickers hardness values between 450 and 650 kgf mm^{-2} have been reported for these coatings in the as-deposited condition [6–8].

Amorphous metallic alloys constitute a new class of materials because of their mechanical, electrical, magnetic, catalytic and corrosion resistance properties which arise from their homogeneous structure. Historically, Kramer obtained the first amorphous alloy in 1934, using the vapor deposition method. Brenner and others obtained the alloys by electrodeposition [9–12].

In a strict sense, all the factors that permit electrodeposition of amorphous alloys are not known. But it seems that the presence of metalloids (P, B and others), which can be codeposited with some transition metals, produce a series of defects, which can provoke distortion in the crystal lattice sufficient to give the material an amorphous character [13, 14]. The results of studies to optimize operational parameters namely, current density, bath temperature, mechanical agitation and pH for the electrodeposition of Ni–W–B amorphous alloys as a function of deposition efficiency and corrosion resistance are reported here.

2. Experimental

The electrochemical bath was prepared using analytical grade chemicals and double distilled, deionized water. The bath used for electrodeposition of the alloy Ni–W–B contained 0.0370 M nickel sulphate, 0.0310 M sodium tungstate, 0.0728 M boron phosphate, 0.0323 M sodium citrate and 0.017 g l^{-1} 1-Na-dodecylsulfate [1]. The bath

pH was adjusted initially and during the deposition process using either ammonium hydroxide or sulfuric acid. The electrodeposition process was usually performed for a period of 2 h.

Prior to the coating deposition the substrate was polished up to 600 grit surface finish. The electrodeposition was performed under galvanostatic control on rotating rectangular copper foil of about 8 cm^2 surface area acting as cathode which was placed inside a cylindrical platinum gauze anode. All specimens were subjected to a series of cleaning stages and finally rinsed in dilute 10% H_2SO_4 to remove any residual alkali.

A potentiostat/galvanostat (Amel 555B) was used to apply a known current density to the cathode. An MTA KUTESZ MD2 thermostat controlled the temperature of the bath and a rotating electrode EG&G PARC 616 (cathode rotation) was used to control mechanical agitation. The Faradaic efficiency was calculated from the charge passed and the weight gained. The alloy composition was taken into account when calculating the deposition efficiency.

A complete factorial design of two levels and four factors (2^4) was used [15], totaling 19 experiments, for a quantitative evaluation of the influence of current density, temperature, mechanical agitation and pH on the alloy deposition efficiency and corrosion resistance (corrosion potential and polarization resistance). Table 1 shows the levels of the factors used, as well as their experimental design codes. Each independent factor was investigated at a high (+1) and a low (−1) level. Runs of center points (0) were included in the matrix and statistical analysis was used to identify the effect of each variable on deposition efficiency and corrosion resistance. Those variables having a major effect on deposition efficiency and corrosion resistance were identified on the basis of confidence levels above 95% ($p < 0.05$). The Software Statistica 5.0 was used for regression analysis of the data.

The potentiodynamic linear polarization (PLP) and electrochemical impedance studies were performed using a potentiostat (Autolab PGSTATE 30) for corrosion analysis. A saturated calomel electrode (Hg/Hg_2Cl_2) and Pt foil were used as reference and auxiliary electrodes, respectively. The PLP curves were obtained with a sweep rate of 1 mV s^{-1} and the impedance experiments were carried out at selected potentials from the PLP curves with a frequency interval of 100 kHz to 0.004 Hz. All the electrochemical corrosion tests were conducted in aqueous 1M NaCl at room temperature.

Table 1. Actual and coded levels of factors studied

Code factors	−1	0	+1
Density/mA cm^{-2}	10	55	100
Temperature/°C	30	50	70
pH	6	8	10
Mechanical agitation/rpm	10	50	90

Characterization of the amorphous structure of the alloy was determined by X-ray diffraction (XRD), using a Siemens D500 Diffractometer, with Cu Kα radiation, a step size of 0.02° and a dwell time of 1 s.

The surface morphology and cross section analysis of the amorphous electrodeposited layers were examined by scanning electron microscopy (SEM) using a Philips XL-30 scanning electron microscope. The composition of the alloy was determined by energy dispersive X-ray analysis (EDX) using a Link Analytical QX-2000 attached to the SEM apparatus.

3. Results and discussion

The results of the electrodeposition efficiency, alloy composition and corrosion resistance (corrosion potential and polarization resistance) obtained from the factorial matrix used to optimize the operational parameters for electrodeposition are presented in Table 2. Atomic absorption spectrometric analysis of all the deposits showed the presence of traces (≈1%) of boron in all the deposits.

The results were subjected to multiple non-linear regression analysis to obtain coefficients for each of the parameters. Estimates of the coefficients with levels higher than 95% ($p < 0.05$) were included in the final model. Deposition efficiency (Eff.), corrosion potential (E_{corr}) and polarization resistance (R_p) can thus be expressed as functions of the independent factors by the linear mathematical model represented by Equations 1, 2 and 3 respectively, where (I) is current density, (pH) is pH and (ω) is rotation rate in rpm. Taking into account only the significant effects, the following equations correspond to the surface response shown in Figures 1 and 2.

$$Eff.(\%) = 29.56 - 17.48I + 5.09\text{pH} - 3.95I^{*}\text{pH} \quad (1)$$

$$E_{\text{corr}} = -0.32238 \quad (2)$$

$$R_p = 9770.5 - 50151I + 3860\omega \quad (3)$$

Analysis of variance showed that these models were significant at a 95% confidence level. The fit of the models was also expressed by the regression coefficient (R^2) equal to 0.94401, 0.81305 and 0.93423 for Eff., E_{corr} and R_p, respectively. The variance and regression analyses demonstrated the statistical significance of the models, justifying the use of a linear model for the statistical analysis.

3.1. *Effect of current density*

The effect of current density on process efficiency was studied in the range 10–100 mA cm^{-2}. Regression analysis of the experimental data showed that current density was the most significant operational factor in

Table 2. Electrodepostion efficiency, corrosion resistance and deposit composition as shown by the factorial matrix

Runs	Current density	Temp.	pH	Mechanical agitation	E_{corr}/V	R_p/Ω	Conc. Ni/≈%wt	Conc.W/≈%wt	Deposition efficiency/%
1	+1	+1	+1	+1	−0.476	9023	74	26	16.10
2	+1	+1	+1	−1	−0.346	16670	76	24	17.65
3	+1	+1	−1	+1	−0.314	4320	92	8	14.07
4	+1	+1	−1	−1	−0.426	3657	91	9	13.46
5	+1	−1	+1	+1	−0.246	12760	89	11	12.58
6	+1	−1	+1	−1	−0.266	8422	93	7	12.65
7	+1	−1	−1	+1	−0.124	1233	91	9	11.77
8	+1	−1	−1	−1	−0.482	5676	92	8	10.55
9	−1	+1	+1	+1	−0.211	21090	71	29	68.06
10	−1	+1	+1	−1	−0.371	4957	76	24	54.95
11	−1	+1	−1	+1	−0.257	19830	91	9	51.57
12	−1	+1	−1	−1	−0.339	6919	92	8	38.05
13	−1	−1	+1	+1	−0.313	35590	73	27	60.87
14	−1	−1	+1	−1	−0.297	7517	81	19	46.50
15	−1	−1	−1	+1	−0.254	7296	91	9	31.28
16	−1	−1	−1	−1	−0.270	14510	83	17	37.20
17	0	0	0	0	−0.460	7666	80	20	21.34
18	0	0	0	0	−0.375	5010	78	22	21.41
19	0	0	0	0	−0.298	4554	79	21	21.66

the electrodeposition process at a 95% confidence level (Equation 1). From this observation and the F test results it can be concluded that the statistical model used in these experiments was representative and reproducible. In contrast, the interactions of current density with rotation rate and temperature were statistically insignificant on the electrodeposition process.

The highest value for the deposition efficiency, approximately 50%, was obtained by using a low current density of 20 mA cm^{-2}. Current densities higher than 80 mA cm^{-2} tended to produce poor quality alloy with the formation of dark deposits [1]. From the experimental data (Table 2) it was observed that a decrease in current density and an increase in temperature increased deposition efficiency. From Equation 3 it can be observed that current density and rotation rate were the factors that most influenced corrosion resistance of the deposit. The best results for corrosion resistance (i.e. corrosion potential and polarization resistance) were obtained with a current density of 35 mA cm^{-2} (Figures 1 and 2). This was associated with a higher deposition of tungsten (Table 2) when compared with the deposits obtained with a current density of 100 mA cm^{-2}. The PLP tests showed the formation of a more efficient passivation film (Figure 3) at a current density 35 mA cm^{-2}.

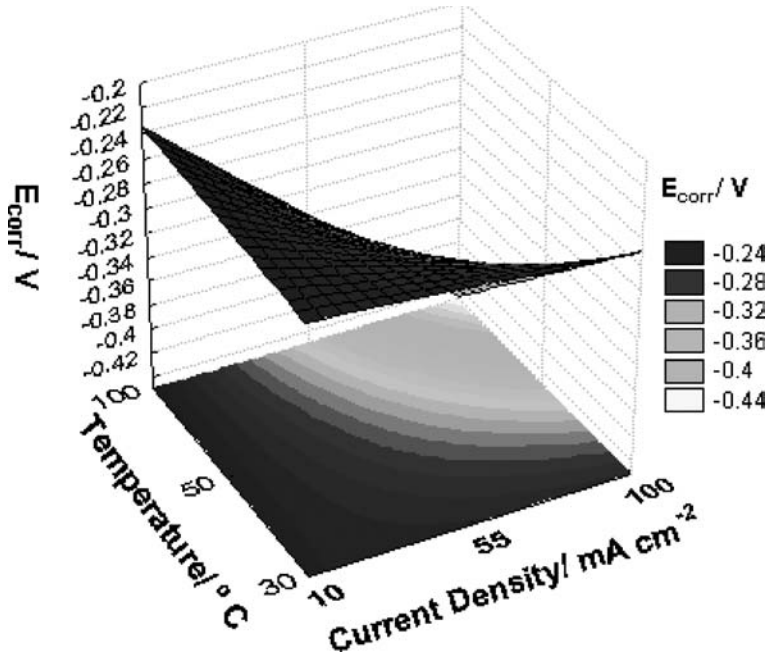

Fig. 1. Fitted surface of influence of current density vs. temperature in relation to corrosion potential of the alloy, using a bath pH of 9.0 and rotation rate at 90 rpm.

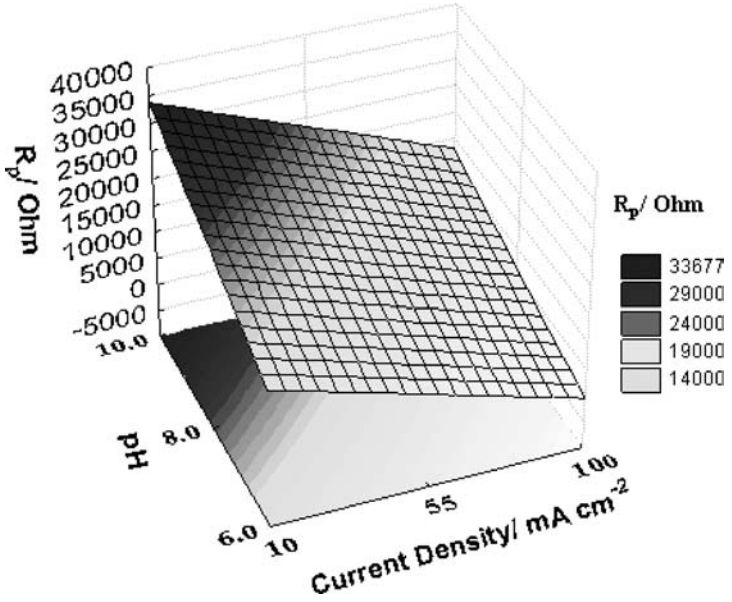

Fig. 2. Fitted surface of influence of current density vs. pH in relation to polarization resistance of the alloy, using a bath temperature of 40 °C and rotation rate at 90 rpm.

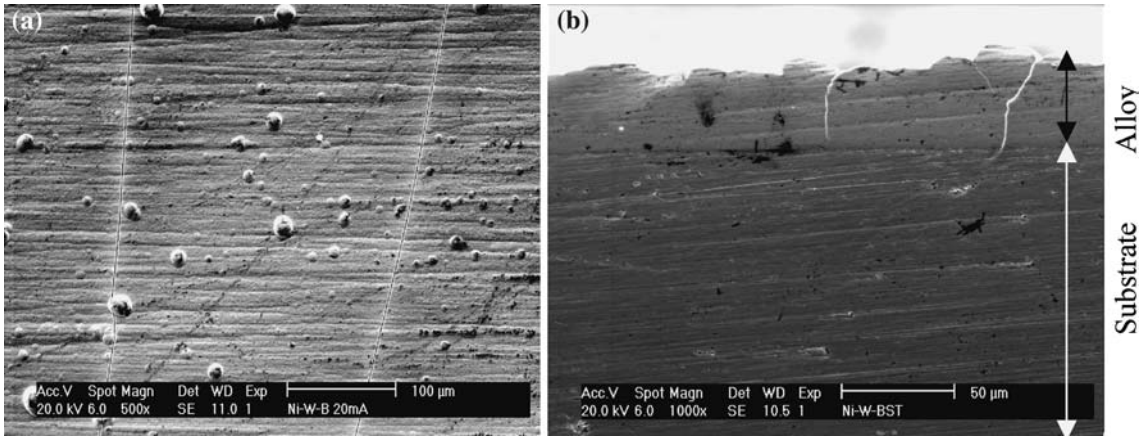

Fig. 3. SEM micrographs of the Ni–W–B alloy (a) surface, with 500× amplification and (b) cross section, with 1000× amplification (current density 20 mA cm^{-2}, temperature 70 °C, pH 9.5 and rotation rate 15 rpm).

3.2. *Effect of temperature*

An increase in temperature usually decreases polarization, increases the concentration of metal at the metal/solution interface and may affect the cathode current efficiency for metal deposition, particularly those deposited from complex ions. The effect of bath temperature on the process efficiency was studied in the temperature range 30–70 °C. From Equation 1, it can be confirmed that the temperature change did not have a statistically significant effect on the process efficiency at the 95% level. Similar results are also reported by Younes and Gileadi [16].

The best results were obtained at 70 °C with a good quality deposit and a deposition efficiency of 50%. The deposits obtained at around 30 °C were of poor quality, with the formation of a dark film with little adherence to the copper substrate [1].

Bath temperature did not have a statistically significant effect on corrosion resistance (Equations 2 and 3). In contrast to the effect of bath temperature on the deposition efficiency, the best temperature for corrosion resistant deposit was between 40 and 50 °C (Figure 1). Deposits obtained at temperatures higher than 60 °C contained high concentrations of nickel, thus decreasing their anti-corrosive proprieties (Table 2).

3.3. *Effect of mechanical agitation*

The mechanical agitation, in this case by cathode rotation, can directly affect the composition of the alloy by reducing the thickness of the diffusion layer at the cathode and by maintaining the concentration of the metal ion adjacent to cathode relatively equal to the concentration in the bulk of the solution. The

concentration of free complexing agent in the cathode diffusion layer is also reduced by agitation, which may have a powerful effect on the potential of one or both of the metals and, hence, on the composition of the deposit. In general, if the concentration of the free complexing agent in the cathode diffusion layer is reduced by agitation of the bath, a corresponding change may occur in the composition of the alloy. These variations in alloy composition are more difficult to predict than those arising from metal ion concentration. The possibility exists that the trend of alloy composition resulting from the reduction in the concentration of free complexing agent may be opposite in sense to that resulting from an increase in the metal ion concentration of the cathode diffusion layer. Such a possibility can occur in an alloy deposition system where only the less noble metal forms a complex with the complexing agent. This means that in baths made up of complex ions, the effects of agitation are not as predictable as those in baths of simple ions.

The effect of mechanical agitation on process efficiency was studied in the range 10–90 rpm. It was observed (Equation 1) that the effect of agitation on alloy deposition efficiency was statistically insignificant whereas apparently a good quality deposit was obtained by agitation at 15 rpm [1].

Mechanical agitation had a statistically significant effect on the corrosion resistance of the alloy at a 95% confidence level (Equation 3). At 90 rpm a good quality corrosion resistant alloy was obtained, this behavior may be correlated with an increase in tungsten content in the deposit at this high rotation rate (Table 2). It was observed that increased rotation rate always increased deposition efficiency and the percentage of tungsten in the deposit (Table 2: runs 9–10 and 13–14) when working at low current densities. This may be ascribed to some degree of mass transport limitation of tungstate species in the bath. The Tungsten content of the alloy was also found to increase with decrease in current density (Table 2: runs 1–9), which is consistent with the above conclusion for mass transport limitation for the rotation rate.

3.4. *Effect of pH*

The pH effect on the deposition efficiency was studied in the pH range 6–10. Regression analysis of the experimental data showed that pH and its interaction with the current density had a significant effect on the process of electrodeposition of the alloy Ni–W–B (Equation 1). With a decrease in current density and an increase in pH the best deposition efficiency obtained was about 50%. The F test confirmed that the statistical model used in these experiments was both representative and reproducible. In contrast to the interaction between pH and current density, the interaction between pH and temperature was statistically insignificant on the electrodeposition process.

The highest deposition efficiency was obtained at pH 9.5, which gave a good quality deposit with desirable adherence and a shiny lustre. At pH values lower than 7.5 a poor quality deposit with a lower Faradaic efficiency was obtained.

The increase in deposition efficiency with increasing pH may be linked to the influence of ammonia in the bath, which may form a complex with the tungstate ions thus rendering them stable in solution. This would obstruct the formation of the mixed metal complex, $[(Ni)(WO_4)(Cit)(H)]^{2-}$, precursor for the deposition of the Ni–W alloy, as proposed by Younes and Gileadi [16].

According to Equations 2 and 3 bath pH did not significantly effect the corrosion characteristics of the deposit. The best values for corrosion resistance were obtained at around pH 9.0, with a good quality deposit and a high concentration of tungsten in the alloy (Table 2). Deposits obtained at pH values below 7.0 contained lower concentrations of tungsten, thus decreasing corrosion resistance.

3.5. *Appearance of the deposit*

Scanning electron microscopy (SEM) showed that the alloy Ni–W–B (Figure 3) deposited on the copper substrate had fewer microcracks, compared to those on the deposits of Co–W–B (Figure 4). The appearance of these micro-cracks can be attributed to the internal stress of tungsten in the deposited material. Similar morphological characteristics for Ni–W alloy were also reported by Yang et al. [17]. A significant increase in the number of the micro-cracks was observed with increase in current density; similar behavior was observed by Donten et al. [18]. Figures 3(b) and 4(b) show that the micro-cracks extend to the copper substrate. Further studies are necessary if micro-cracks on the alloy surface are to be eliminated or greatly reduced so as to improve corrosion resistance. The deposit was uniformly granular across its surface.

The deposit also showed good adherence and lustre, with an average thickness of 32 μm after 2 h of electrodeposition. The composition of the electro-deposited alloy was obtained with the help of EDX (Table 2).

The amorphous character of the alloy was confirmed by X-ray diffraction analysis (XRD); a single broad peak confirmed the amorphous structure of the alloy. Boron was added to the bath in the form of boron phosphate, which was co-deposited with the Ni–W alloy, producing an amorphous structure and, consequently, interesting properties such as a high level of hardness. Similar behavior was observed by Wikiel and Osteryoung [19].

3.6. *Corrosion resistance*

Figures 5 and 6 show the potentiodynamic curves obtained for the alloys Co–W–B, Ni–W–B(Eff.) deposited under optimal conditions for deposition efficiency

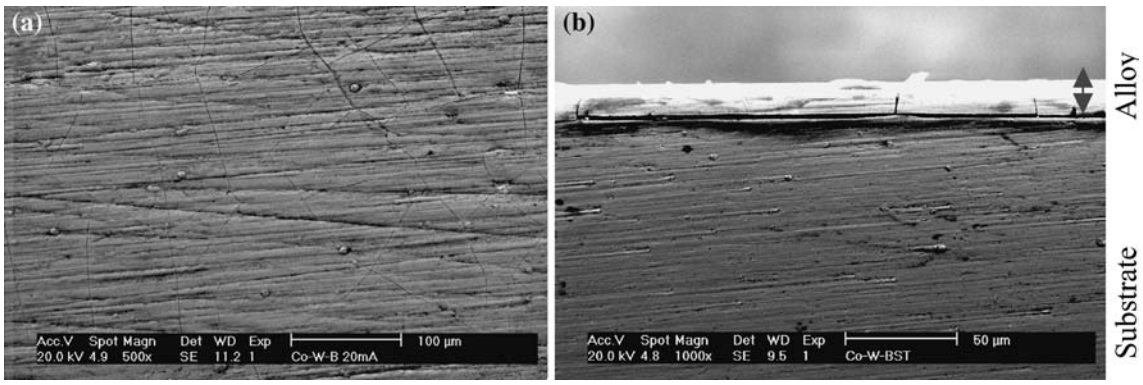

Fig. 4. SEM micrographs of the Co–W–B alloy (a) surface, with 500× amplification and (b) cross section, with 1000× amplification (current density 20 mA cm^{-2}, temperature 70 °C, pH 9.5 and rotation rate 90 rpm).

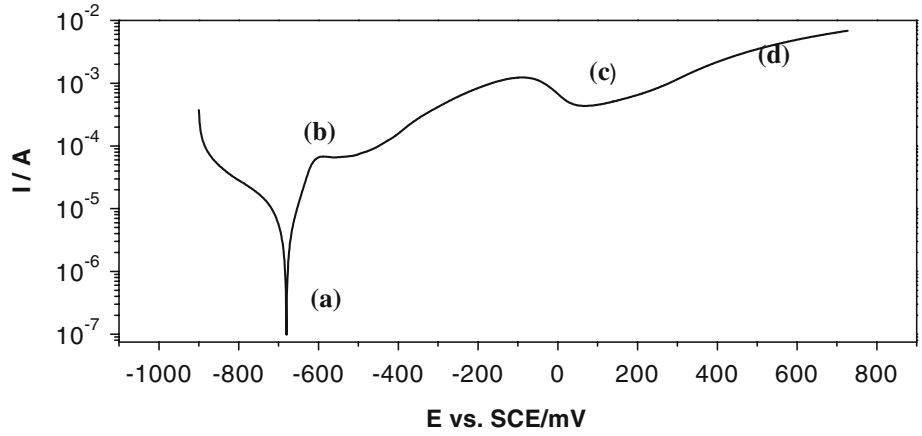

Fig. 5. Anodic polarization curve of Co–W–B alloy (current density 20 mA cm^{-2}, temperature 70 °C, pH 9.5 and rotation rate 90 rpm).

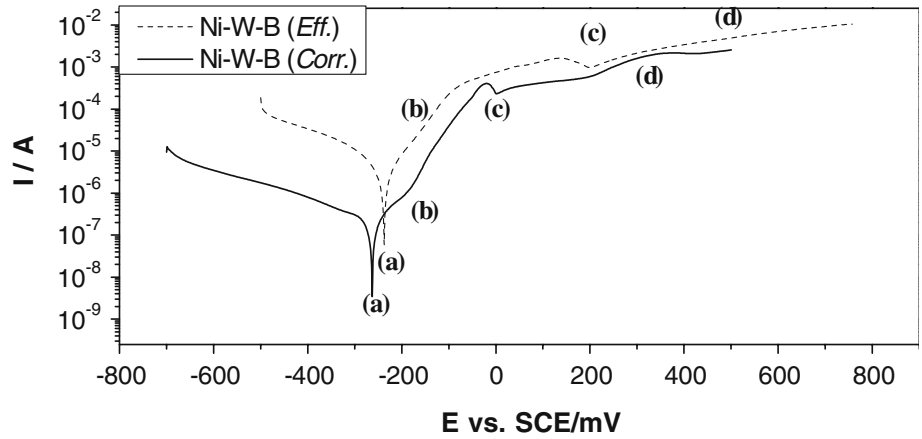

Fig. 6. Anodic polarization curve of Ni–W–B(Eff.) at cathode current density 20 mA cm^{-2}, bath temperature 70 °C, pH 9.5, mechanical agitation 15 rpm; and Ni–W–B(Corr.) at a current density 35 mA cm^{-2}, temperature 40 °C, pH 9.0, rotation rate 90 rpm.

and Ni–W–B(Corr.) deposited under optimal conditions for corrosion resistance in 1 M NaCl. The electrodeposits containing Ni [Ni–W–B(Eff.) and Ni–W–B(Corr.)] had corrosion potentials (approximately 450 mV and 290 mV, respectively) more positive than that of the electrodeposit containing Co. Additionally, the anodic branch of the polarization curves for the three studied alloys were similar, showing a decrease in current (point c) suggesting the formation of a passive film on the alloy surface. However, the film is not stable in this medium, as the current increases again rapidly with increase in potential. Both the alloys show dissolution of the protective film at point (d). The analysis also reveals that both Ni alloys are more corrosion resistant than the Co–W–B alloy (Table 3).

Table 3. Corrosion data obtained from potentiodynamic polarization curves

Corrosion data	Co–W–B	Ni–W–B(Eff.)	Ni–W–B(Corr.)
E_{corr}/V	−0.680	−0.238	−0.300
R_p/Ω	3.357×10^3	5.569×10^3	3.369×10^4

Electrochemical impedance experiments were carried out to obtain information about the passivation behavior of Ni–W–B and Co–W–B alloys. The impedance measurements were performed in the regions a–d marked on the polarization curves of Figures 5 and 6.

Figure 7 shows the impedance diagram, which represents the corrosion potential correlated to point (a). Figures 8, 9 and 10 correlate with the potentials represented by (b), (c) and (d), respectively.

The Ni–W–B alloys had higher impedance values than the Co–W–B alloy, thus confirming the higher corrosion resistance of the former. Additionally, Figure 7 shows a typical diagram for a charge transfer process at the interface, indicating that surface reactions already occur at the corrosion potential. Figures 8 and 9 show typical diagrams for the process of passivation and dissolution that confirm the findings of the polarization curves, which suggested the presence of an unstable passive film on the surface. The same type of passivation and dissolution process was also observed by Keddam et al. [20]. Figure 10 shows the impedance diagrams, which are associated with transpassivation and may be attributed to dissolution of the passive film as also observed by Keddam et al. [21]. By the end of the impedance tests on the Co–W–B alloy, almost complete dissolution of the electrodeposited film occurred, exposing the copper substrate. In the case of Ni–W–B alloy, which was exposed to the same corrosion medium and for the same period, the copper substrate surface did not become visible. This behavior is associated to the dissolution process presented in Figure 10.

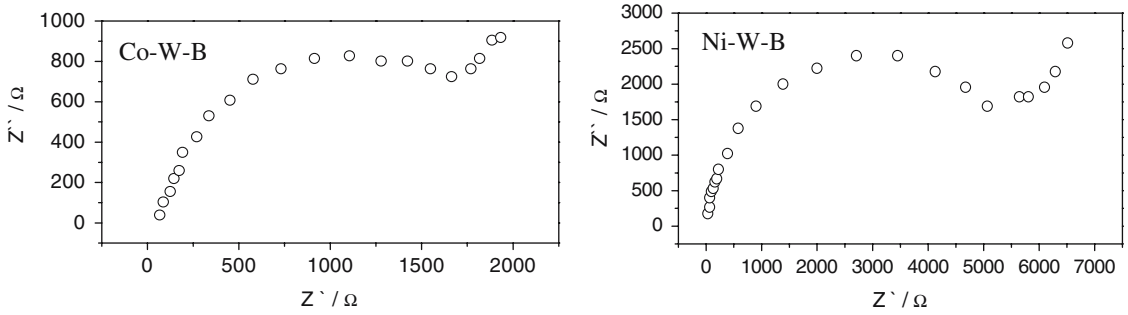

Fig. 7. Impedance diagrams related to the point (a) of the anodic polarization curves of Co–W–B and Ni–W–B alloys.

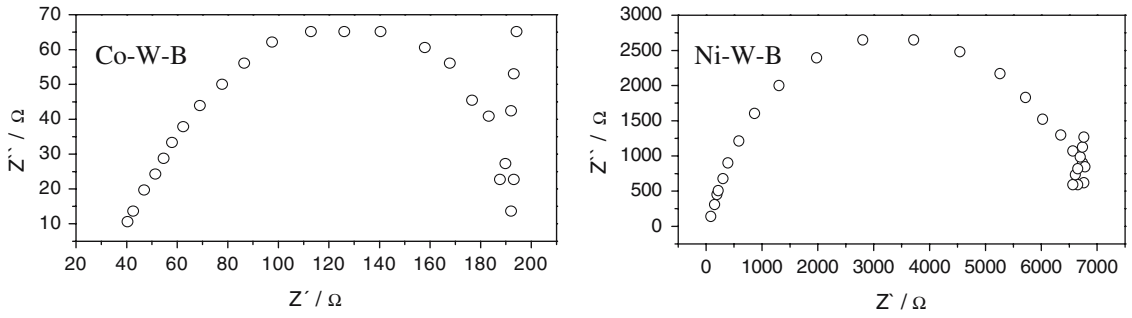

Fig. 8. Impedance diagrams related to the point (b) of the anodic polarization curves of Co–W–B and Ni–W–B alloys.

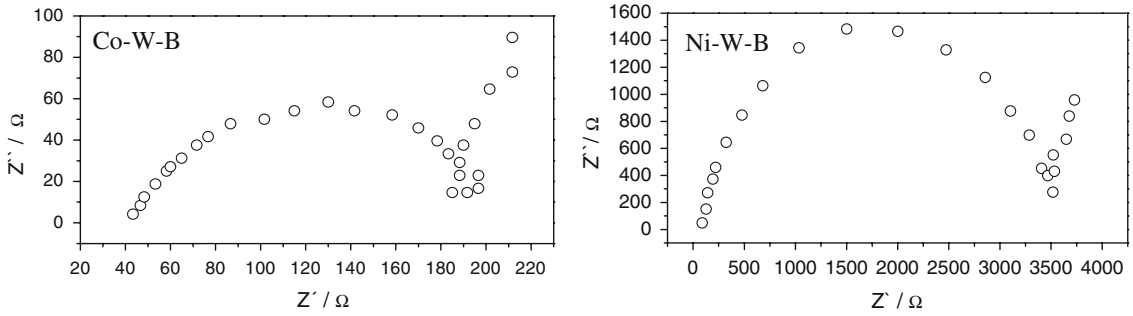

Fig. 9. Impedance diagrams related to the point (c) of the anodic polarization curves of Co–W–B and Ni–W–B alloys.

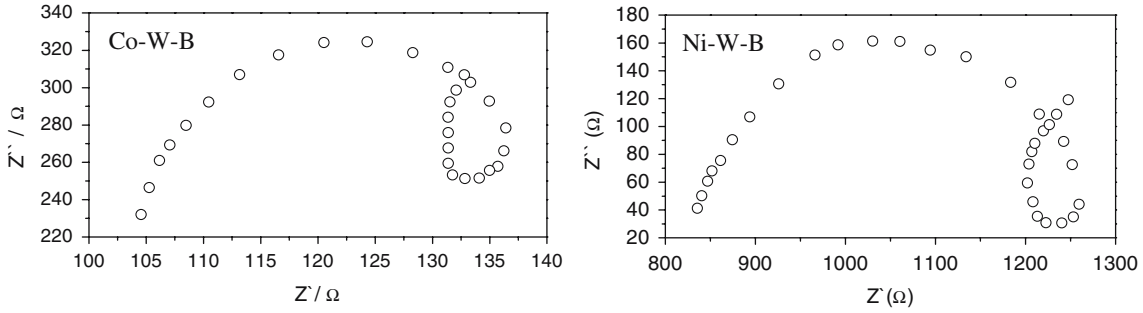

Fig. 10. Impedance diagrams related to the point (d) of the anodic polarization curves of Co–W–B and Ni–W–B alloys.

The Co–W–B alloy used in this study was obtained using a current density of 20 mA cm^{-2}, at 70 °C, with a pH of 9.5 and rotation rate at 90 rpm which gave a deposition efficiency of about 30%. The average composition of the deposit was 60 wt% Co, 40 wt% W with traces of boron giving a corrosion potential of −0.680 V and a polarization resistance of 3.357×10^3 Ω.

The conditions for efficient deposition of the Ni–W–B(Eff.) alloy were a current density 20 mA cm^{-2}, at 70 °C, with a of pH 9.5 but with rotation rate at 15 rpm, which gave a deposition efficiency of about 50%. The average composition of the deposit was 83 wt% Ni, 16 wt% W with traces of boron, giving a corrosion potential of −0.238 V and a polarization resistance of 5.569×10^3 Ω. Similar corrosion characteristics of a Ni–W alloy are also reported by Yang et al. [17].

For depositing a good quality corrosion resistant alloy [Ni–W–B(Corr.)] a current density of 35 mA cm^{-2} was required at a temperature of 40 °C, pH 9.0 and rotation rate at 90 rpm. This gave a deposition efficiency of about 38%, with an average deposit composition of 73 wt% Ni, 27 wt% W and traces of boron. The corrosion potential was −0.300 V and the polarization resistance 3.369×10^4 Ω. Even though the corrosion potential was not particularly good the deposit obtained under these operational conditions showed high polarization resistance and, consequently, a low dissolution rate, thus confirming its corrosion resistance.

4. Conclusions

For the optimized bath composition and within the range of operating parameters studied it can be affirmed that:

1. For electrodeposition of the alloy Ni–W–B at an efficiency of 50% the optimized values of operational parameters were: cathode current density 20 mA cm^{-2}, bath temperature 70 °C, pH 9.5 and rotation rate at 15 rpm.
2. Good deposits in terms of corrosion resistance were obtained under the following operational conditions: current density 35 mA cm^{-2}, bath temperature 40 °C, pH 9.0 and rotation rate at 90 rpm giving a deposition efficiency of 38%.
3. The deposits obtained under optimum conditions for both deposition efficiency and corrosion resistance were of an amorphous nature. These deposits had micro-cracks on their surfaces, which reached down to the copper substrate. Further studies are required to determine how these micro-cracks might be eliminated.

Acknowledgements

The authors are grateful to CNPq, CAPES and FINEP for financial assistance and to PRH-25/ANP/MCT for a fellowship to one of the authors (RACS), to FUNCAP for a scholarship to G. P. da Silva and to Howard W. Pearson for his valuable contribution in this work.

References

1. R.A.C. Santana, S. Prasad and F.S.M. Santana, *Eclética Química*. **28** (2003) 69.
2. S.M. Mayanna, N. Nunichandraiah and T. Mimani, *J. Appl. Electrochem.* **23** (1993) 339.
3. A.T. Wasko, *Electrochemistry of Tungsten and Molybdenum* (Naukova dumka, Kiev, 1977).
4. A. Brenner, *Electrodeposition of Alloy*, vol. 2 (Academic Press, New York, 1963), pp. 589.
5. B.N. Maruthi, L. Ramesh, S.M. Mayanna and D. Landolt, *Plating Surf. Finish.* **86** (1999) 85.
6. S. Prasad, F.S.M. Santana and F.A. Marinho, *Braz. J. Chem. Eng.* **17** (2000) 423.
7. S. Eskin, O. Berkh, G. Rogalsky and J. Zahavi, *Plating Surf. Finish.* **85** (1998) 79.
8. M. Donten and Z. Stojek, *J. Appl. Electrochem.* **26** (1996) 665.
9. C. Gangmin, Y. Fangzu, H. Ling, N. Zhenjiang, X. Shukai and Z. Shaomin, *Trans. IMF* **79**(2) (2001) 81.
10. J. Kramer, *J. Annln. Phys.* **19** (1934) 37.
11. A. Brenner, D.E. Couch and E.K. Williams, *J. Res. Natl. Bur. Standards* **44** (1950) 109.
12. F.A. Marinho, F.S.M. Santana, A.L.S. Vasconcelos, R.A.C. Santana and S. Prasad, *J. Braz. Chem. Soc.* **13** (2002) 522.
13. U. Admon and M.P. Dariel, *J. Appl. Phys.* **59**(6) (1986) 2002.
14. P. Schloßmacher and T. Yamsaki, *Mikrochim. Acta* **132** (2000) 309.
15. L.A.M. Ruotolo and J.C. Gubulin, *J. Appl. Electrochem.* **33** (2003) 1217.
16. O. Younes and E. Gileadi, *Electrochim. Acta* **48** (2003) 2551.

17. F-Z. Yang, Y-F. Guo, L. Hung, S-K. Xu and S-M. Zhou, *Chinese J. Chem.* **22** (2004) 228.
18. M. Donten, H. Cesiulis and Z. Stojek, *Electrochim. Acta* **45** (2000) 3389.
19. W. Wikiel and J. Osteryoung, *J. Appl. Electrochem.* **22** (1992) 506.
20. M. Keddam, O.R. Mattos and H.J. Takenouri, *J. Electrochem. Soc.* **128** (1981) 257.
21. M. Keddam, J.F. Lizee, C. Pallotta and H.J. Takenouri, *J. Electrochem. Soc.* **131** (1984) 2016.